

Synthesis and Fluorescence Quenching Study of the Novel Cationic Probe Derived from Luminarosine

by Grażyna Wenska, Bohdan Skalski¹⁾, Iwona Tomska-Foralewska, and Stefan Paszyc

Faculty of Chemistry, A. Mickiewicz University, PL-60-780 Poznań

Dedicated to Professor *André M. Braun* on the occasion of his 60th birthday

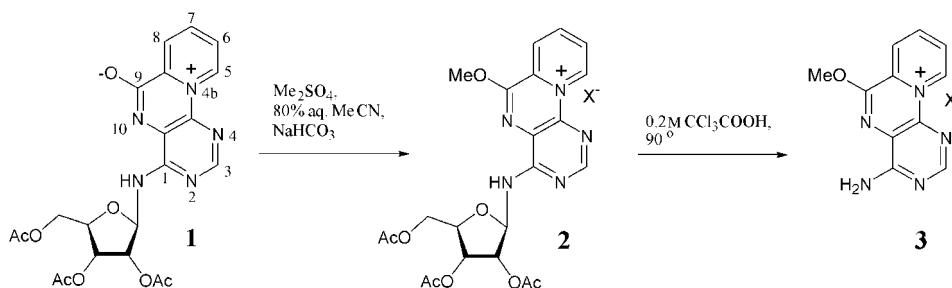
A simple and efficient transformation of the zwitterionic luminarosine into a brightly fluorescent cationic analogue, namely 1-amino-9-methoxy-2,4,10-triaza-4b-azoniaphenanthrene (**3**), is reported. The fluorescence quenching of **3** by common nucleotides, calf-thymus (CT) DNA, and halide ions was investigated by means of spectrophotometric and spectrofluorometric methods. Intermolecular static and dynamic fluorescence-quenching constants for quenching of **3** by nucleotides and halide ions were determined in aqueous solution. Evidence for formation of nonfluorescent ground-state complexes of **3** with nucleotides and CT-DNA is presented. *Scatchard* analysis of the CT-DNA quenching data resulted in a binding constant of $2.8 \times 10^4 \text{ M}^{-1}$ and a number of binding sites per base pair of 0.049.

Introduction. – Brightly fluorescent 1-[(2',3',5'-tri-*O*-acetyl- β -D-ribofuranosyl)amino]-2,4,10-4b-azoniaphenanthrene-9-olate (**1**), termed tri-*O*-acetyl luminarosine [1], which has excitation and emission maxima at 430 and 530 nm in aqueous solution, belongs to a rather limited number of modified nucleosides that absorb and emit light in the visible region. The attractive photophysical properties of this compound [2], as well as its chemical stability under oligonucleotide-synthesis conditions, make it an excellent candidate for a fluorescent probe of nucleic acids and other biological systems. Sequence-specific introduction of this fluorophore into oligodeoxynucleotides has already been achieved [3]. Recent studies on fluorescence quenching of the parent de-*O*-acetylated nucleoside (luminarosine) and the aglycone (luminarine) by I^- ions in living cells revealed the great potential of the former as a long-wavelength iodide-sensitive fluorescent indicator for measurements of the cystic fibrosis transmembrane-conductance regulator (CFTR) gene expression in cells [4]. The high intracellular fluorescence of the luminarosine, combined with its red-shifted emission and I^- selectivity, make it superior to quinolinium-based halide indicators and indicates its possible application in the high-throughput screening of compounds for correction of the cystic fibrosis phenotype. Encouraged by these findings, we have undertaken the synthesis and detailed photophysical studies of some analogues of the luminarosine modified within the chromophoric part in the hope of obtaining fluorophores of different and possibly improved photophysical properties. In this communication, we present the simple and efficient transformation of the zwitterionic luminarosine into another very bright fluorophore, namely its cationic analog, 1-amino-9-methoxy-2,4,10-triaza-4b-azoniaphenanthrene (**3**). The spectral properties as well as the results of a fluorescence-quenching study of **3** by common nucleotides and halide ions is discussed.

¹⁾ Phone: (48-51)8291 1351; fax: (48-61)865 8008; e-mail: bskalski@amn.edu.pl.

Results and Discussion. – *Synthesis and Spectral Characteristics of 3.* Tri-*O*-acetyluminarosine (**1**) was prepared starting from tri-*O*-acetylinosine in a multistep synthesis involving photochemical transformation of the intermediate *N*-[9-(2',3',5'-tri-*O*-acetyl- β -D-ribofuranosyl)purin-6-yl]pyridinium chloride as described in [5]. Methylation of **1** with Me_2SO_4 in 80% aqueous MeCN in the presence of NaHCO_3 for 12 h, followed by treatment of the resulting methylated nucleoside with 0.2M CCl_3COOH for 3 h at 90° , gave the desired cationic derivative **3** (*Scheme*). The crude product was subjected to reversed-phase column chromatography and subsequent ion exchange on *Dowex* (Cl^-) to give chromatographically pure **3** as the Cl^- salt ($\text{X} = \text{Cl}^-$) with 87% overall yield. The elemental composition of **3** was confirmed by HR-LSIMS and elemental analysis. The assignment of proton signals in the $^1\text{H-NMR}$ spectrum was straightforward by COSY and by comparison of chemical shifts with those reported previously for the luminarine in acidic medium ($\text{CD}_3\text{OD} + \text{CD}_3\text{COOD}$) [1]. Both chemical-shifts arguments and $^1\text{H},^{13}\text{C}$ -HETCOR experiments were used for assignments of the signals in the $^{13}\text{C-NMR}$ spectrum of **3**. In agreement with proposed structure of **3** the Me protons lead to a NOE with H–C(8), and a long-range coupling $^3J(\text{C,H})$ with C(9) is observed. The chloride **3** is chemically stable over a wide pH range from strongly acidic to moderately basic (pH 9.0) conditions. However, at higher pH, slow demethylation with formation of the luminarine, *i.e.*, the aglycone of **1**, occurs.

Scheme



The UV absorption and fluorescence data for **3**, including fluorescence quantum yields and lifetimes in H_2O , MeCN, and MeOH, are collected in *Table 1*; for the sake of comparison, the respective data for the luminarine in H_2O , are also included. The photophysical properties of the latter are virtually identical to those of the luminarosine [2]. As can be seen, **3** is twice as efficient a fluorophore as the parent luminarine, with the fluorescence quantum yield reaching 100%. Both the absorption and fluorescence maxima of **3** are *ca.* 40 nm blue-shifted compared to those of the luminarine. In the case of the latter, a similar blue shift in the long-wavelength absorption maximum was observed upon protonation in acidic solution; however, this was accompanied by substantial reduction in the fluorescence intensity [2]. Unlike luminarine, which displays a large negative solvatochromism, solvent has little effect on the fluorescence quantum yield and lifetime of **3**, and only a small red shift in absorption and fluorescence maxima with decreasing solvent polarity is observed.

Fluorescence Quenching. Small fluorescent molecules that can bind to DNA attract much attention due to their potential use in various areas of nucleic acids studies [6].

Table 1. Absorption and Fluorescence Maxima, Quantum Yields and Lifetimes of **3** in Various Solvents

Compound	Solvent	Absorption		Fluorescence		
		λ_{\max} [nm]	ϵ [M ⁻¹ cm ⁻¹]	λ_{\max} [nm]	φ	τ [ns]
Luminarine ^{a)}	H ₂ O	428	9000	533	0.47	7.3
(3)	H ₂ O	390	6800	489	0.99	10.0
(3)	MeCN	393	6400	492	0.99	10.0
(3)	MeOH	400	6400	502	0.91	10.1

^{a)} Taken from [2].

The significant structural similarity of **3** to some heterocyclic cations that bind to specific DNA sequences [7] combined with extremely bright fluorescence make it a good candidate for a DNA probe. To test the interaction of **3** with common nucleic acid bases, its absorption and emission spectra as well as fluorescence lifetimes were measured in the presence of nucleoside-5'-monophosphates (AMP, GMP, UMP, and CMP). Generally, increasing the concentration of the nucleotides up to 0.05M resulted in a small decrease in the intensity and a red shift of the long-wavelength absorption band of **3**, with a concomitant decrease in the fluorescence intensity but without any change in the shape and position of the emission band. As an example, changes in the UV absorption and fluorescence-emission spectra of **3** in the presence of increasing concentrations of GMP are shown in *Fig. 1*. Both the magnitude of the UV spectral changes and the extent of the fluorescence quenching depended on the type of the nucleotide. *Fig. 2* shows *Stern-Volmer* plots for GMP quenching of **3**. The plot obtained from quantum yields clearly displays upward curvature, whereas that obtained from fluorescence lifetimes is linear over the entire range of GMP concentrations and shows much less quenching than the former. Similar behavior was also observed for quenching of **3** by the remaining three nucleotides. Such behavior is typical for cases where both the dynamic (collisional) and static fluorescence-quenching processes operate. The lack of any additional emission in the presence of the nucleotides, as indicated by the spectral identity of the quenched emissions with that of unquenched, as well as the single-exponential decays across all quencher concentrations, allow us to assume that the ground-state interactions between **3** and nucleotides are responsible for complete quenching of the fluorophore. To estimate the relative contributions of the static and dynamic components to the overall quenching for all nucleotides, a modified form of *Stern-Volmer* equation (*Eqn. 1*) [8] was used:

$$\frac{F_0}{F} = (1 + K_D[Q])(1 + K_S[Q]) \quad (1)$$

The dynamic *Stern-Volmer* constants K_D , which are defined by *Eqns. 2* and *3*:

$$\frac{\tau_0}{\tau} = 1 + K_D[Q] \quad (2)$$

$$K_D = k_q\tau_0 \quad (3)$$

were determined from the lifetime plots and then the static constants K_s , corresponding to the association constants of a nonfluorescent 1:1 ground-state complexes, were obtained by plotting:

$$\frac{F_0}{F} / (1 + K_D[Q]) \text{ vs. } [Q] \quad (\text{cf. Fig. 3}).$$

The calculated K_D and K_S constants as well as the bimolecular quenching rate constant k_q for all the nucleotide quenchers are summarized in Table 2.

As can be seen, both the static and dynamic fluorescence-quenching constants increase in the order $\text{UMP} < \text{CMP} \ll \text{AMP} < \text{GMP}$ and, in the case of GMP, for which $K_s > K_D$, the overall quenching process is dominated by the static component. Taking into account that static quenching is frequently observed in fluorophores that engage in stacking interactions with purine and pyrimidine nucleotides [9], one can assume that the above order of increasing K_s values reflects the increasing tendency of the

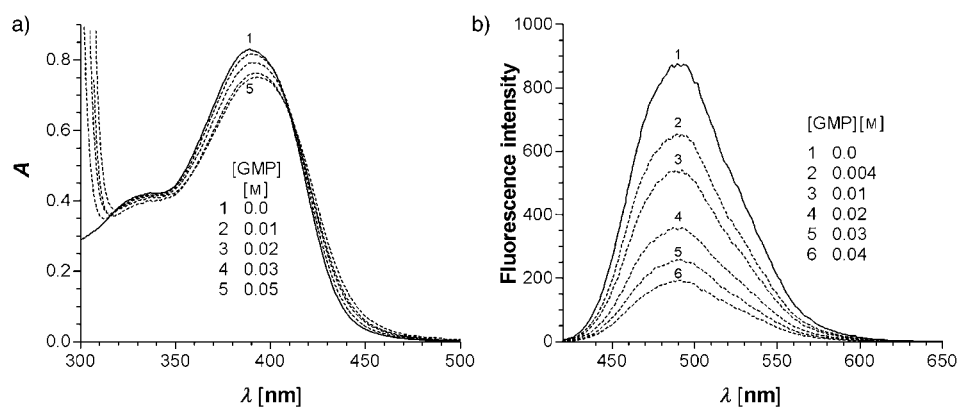


Fig. 1. Changes in the a) absorption and b) fluorescence spectra of **3** in the presence of GMP (in 0.05M cacodylic buffer, pH 7.0)

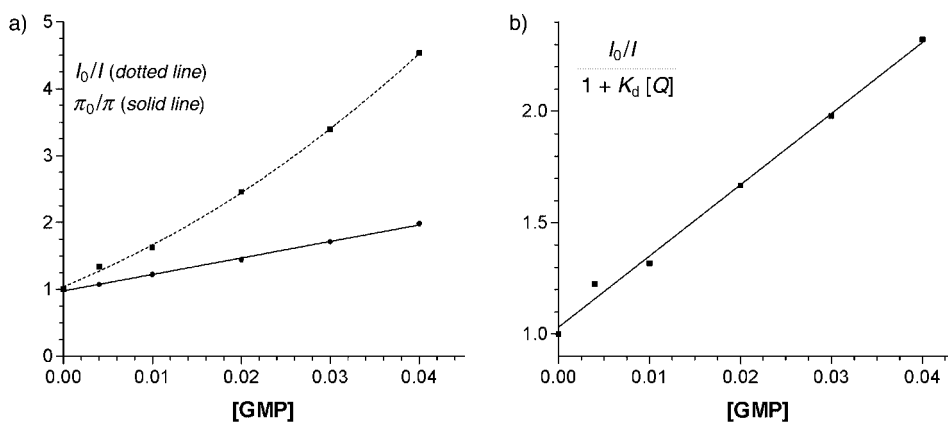


Fig. 2. Fluorescence quenching of **3** by GMP. a) The intensity and the lifetime Stern-Volmer plots, and b) the modified Stern-Volmer plot. The excitation wavelength used was that of the isobestic point at 415 nm.

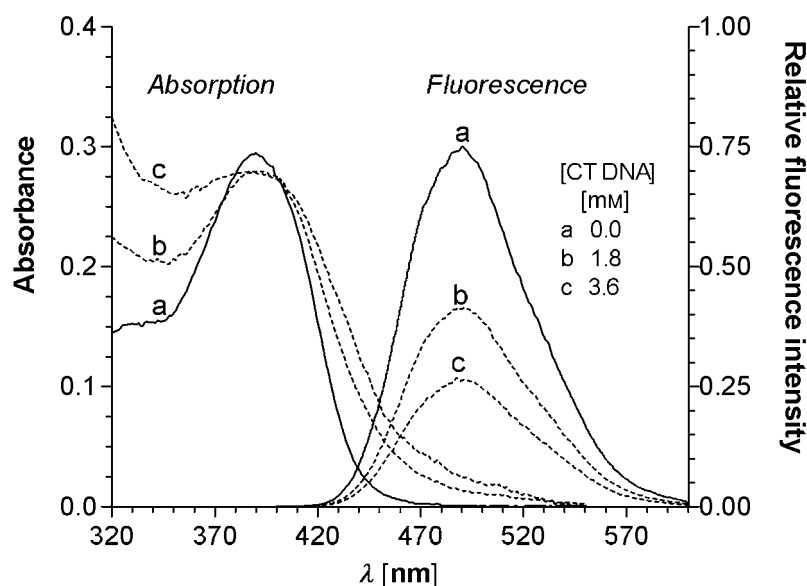


Fig. 3. Absorption and fluorescence spectra of **3** (3.75×10^{-5} M) in the presence of CT-DNA (0–3.6 mM per nucleotide; in 0.05M cacodylic buffer pH 7.0)

Table 2. Static K_s and Dynamic K_D Stern-Volmer Constants and Bimolecular Quenching constants k_q for Quenching of **3** by Nucleoside-5'-monophosphates (in 0.05M cacodylic buffer, pH 7.0).

Quencher	K_s [M^{-1}]	K_D [M^{-1}]	$k_q \times 10^{-9}$ [$M^{-1}s^{-1}$]
UMP	4.1 ± 0.3	7.6 ± 0.2	0.90
CMP	7.7 ± 0.8	12.6 ± 1.96	1.99
AMP	19.2 ± 0.8	19.6 ± 2.5	2.30
GMP	32.0 ± 1.2	24.6 ± 0.6	2.90

nucleotides to display ground-state stacking interactions with **3**. The calculated k_q values, which reflect the quenching efficiencies, fall into the range expected for the diffusion-controlled rates and increase in the order that coincides with the sequence of decreasing oxidation potentials of the bases in nucleotides ($U > C > A > G$) [10]. This is a clear indication that the quenching mechanism involves electron transfer from the nucleotides to the excited fluorophore.

Fig. 4 shows the absorption and fluorescence spectra of **3** ($37.5 \mu M$) recorded in the presence of CT-DNA (0–3.6 mM in bp). As can be seen, increasing amounts of CT-DNA result in a red shift and significant broadening of the long-wavelength absorption band with concomitant decrease in the fluorescence intensity, but without any change in the shape of the emission band. However, unlike in the case of the nucleotides, the fluorescence lifetime of **3** remained unchanged over the entire range of CT-DNA concentrations. The fluorescence-quenching constant evaluated from the Stern-Volmer plot (Fig. 4) amounts to $528 M^{-1}$ of DNA phosphates and is *ca.* 16 times greater than that for GMP, which is the most effective quencher of all the nucleoside monophosphates (see above). These observations indicate that the quenching is entirely

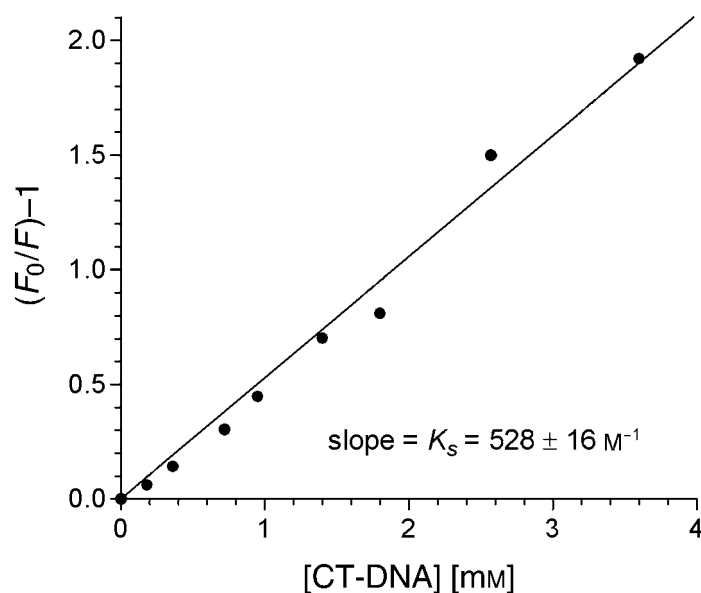


Fig. 4. Stern-Volmer quenching plot of **3** with increasing concentration of CT-DNA with excitation at the wavelength of the isosbestic point at 402 nm

static and results from strong electronic interactions between the fluorophore and the DNA bases in a ground-state fluorophore CT-DNA complex. The fluorescence quenching data were also analyzed in terms of the *Scatchard* equation (*Eqn. 4*) [11]:

$$\frac{r}{C_f} = nK - rK \quad (4)$$

where r is the ratio of bound fluorophore (C_b) to the DNA base-pair concentration, C_f is the concentration of free fluorophore, n is the maximum value of r (*i.e.*, the maximum number of binding sites per DNA base pair), and K is the intrinsic binding constant of the fluorophore. The concentration of the free dye was determined from *Eqn. 5*:

$$C_f = \frac{F}{F_0} \times C_f^0 \quad (5)$$

where F_0 and F are the fluorescence intensities in the absence and in the presence of DNA, respectively, and C_f^0 is the concentration of the fluorophore added. The amount of bound probe was equal to $C_f^0 - C_f$.

Scatchard plot of the above fluorescence titration data displays good linearity (*cf. Fig. 5*) and results in a binding constant (K) of $2.8 \times 10^4 \text{ M}^{-1}$ and a number of binding sites per base pair (n) of 0.049 corresponding to *ca.* 20 base pairs per binding site. These parameters are several times lower than those reported for strongly binding, intercalating dyes such as methylene blue [12], proflavine, or ethidium bromide [13], and indicate rather moderate binding affinity of **3** to DNA. Although the observed

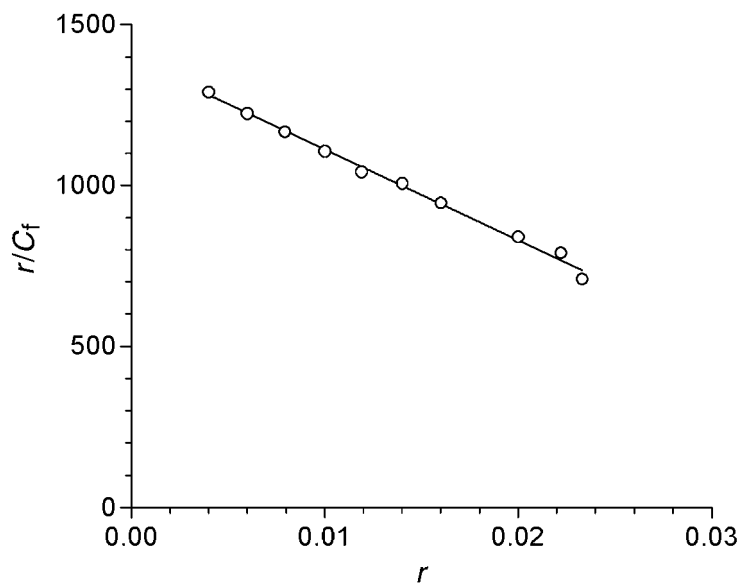


Fig. 5. Scatchard plot of the fluorescence titration of **3** with CT-DNA

hypochromism, broadening, and red shift of the absorption band, as well as efficient quenching of the latter upon binding to DNA are indicative of intercalation [14], the unequivocal identification and characterization of the binding mode of **3** requires further investigation.

Among the halide ions, only I^- and, to a lesser extent, Br^- ions quench the fluorescence of **3**. The relevant *Stern-Volmer* plots are shown in Fig. 6. The plot obtained on the basis of steady-state intensity data for I^- quenching shows an upward curvature at higher quencher concentrations, whereas that constructed from the lifetime data is linear and gives $k_q\tau = 105 \text{ M}^{-1}$, from which a value of $k_q = 10.2 \times 10^9 \text{ M}^{-1}\text{s}^{-1}$ is calculated. This value is almost an order of magnitude greater than that obtained for I^- quenching of the parent luminarosine [2], reflecting the cationic character of **3**. The higher sensitivity of the latter to halide-ion quenching is also reflected in its susceptibility to Br^- quenching, not observed in the case of luminarosine. The steady-state fluorescence for Br^- quenching of **3** is linear and coincides with the corresponding lifetime plot indicating that the quenching is entirely dynamic. The values of $k_q\tau = 69 \text{ M}^{-1}$ and $k_q = 6.7 \times 10^9 \text{ M}^{-1}\text{s}^{-1}$ were obtained from the plots for Br^- quenching.

Conclusions. – The fluorescence of **3** is quenched by common nucleotides both in collisions and by formation of weak, nonfluorescent ground-state complexes. The correlation between the increasing order of the nucleotide quenching efficiency and the sequence of decreasing oxidation potentials of the bases in nucleotides ($U > C > A > G$) indicates an involvement of photoinduced electron transfer in the quenching mechanism. In the presence of CT-DNA, the fluorescence of **3** is quenched exclusively due to the nonfluorescent complex formation. *Scatchard* analysis of the fluorescence-

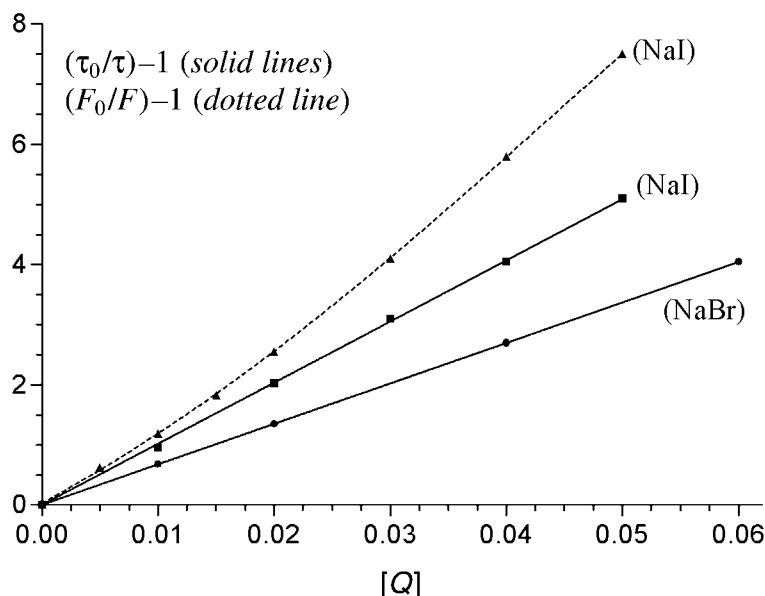


Fig. 6. Stern-Volmer plots for NaI and NaBr quenching of **3**. The excitation wavelength used was that of the isosbestic point at 415 nm

quenching data indicates moderate binding affinity of **3** to DNA, however the results do not allow us to identify the mode of binding.

Experimental Part

General. Tri-*O*-acetyluminarosine (**1**) was prepared as described in [5]. Nucleoside 5'-monophosphates (AMP, GMP, CMP, UMP) as well as the sample of calf-thymus deoxyribonucleic acid (CT-DNA) were purchased from Sigma Chemical Co. UV Spectra: Perkin-Elmer Lambda 17 spectrophotometer; λ_{\max} in nm (ϵ). ^1H - and ^{13}C -NMR: δ in ppm. Fluorescence emission spectra: Perkin-Elmer Lambda 17 and LS50B instruments, resp., emission spectra were corrected for instrumental distortion. Fluorescence quantum yields were determined relative to quinine sulfate as a standard ($\varphi = 0.51$ in 0.1M H_2SO_4) [15]. Fluorescence lifetimes were measured on an IBH model 5000 single-photon-counting spectrometer equipped with a H_2 -filled ns flash lamp 5000F (1.2 ns width at half-maximum of the excitation pulse) as the excitation source. The exper. decay curves were deconvoluted with an IBH Consultants Version 4 software. Fluorescence quenching exper. with nucleotides and CT-DNA were performed in 0.05M cacodylic buffer (pH 6.5) under aerobic conditions. In the case of quenching by nucleoside monophosphates, the solns. were prepared by mixing the same amount of stock soln. of the fluorophore with increasing amounts of the solns. of nucleotides, whereas, in the case of CT-DNA titrations, samples were prepared by mixing various proportions of the fluorophore and the DNA stock solns. while maintaining the total volume of the mixture constant (1 ml). DNA Concentrations per nucleotide were determined by UV-absorption spectroscopy, based on a molar extinction coefficient of $6600 \text{ M}^{-1}\text{cm}^{-1}$ at 260 nm [16]. The solns. used in the quenching exper. with halide ions were prepared from aq. stock solns. of the fluorophore, NaCl, NaBr, NaI, and NaClO_4 , so as to maintain a constant ionic strength.

Synthesis of 1-Amino-9-methoxy-2,4,10-triaza-4b-azoniaphenanthrene Chloride (3). Tri-*O*-acetyluminarosine (**1**; 0.471 g, 1 mmol) was dissolved in 80% aq. MeCN (20 ml). Then, solid NaHCO_3 (1.01 g, 12 mmol) and Me_2SO_4 (0.63 g, 5 mmol) were added, and the mixture was stirred at r.t. When the starting nucleoside was completely consumed (ca. 12 h, by HPLC), the mixture was filtered, and the filtrate evaporated to dryness. The residue was dissolved in 30 ml of 0.1M aq. soln. of CCl_3COOH , and the mixture kept at 95°. As revealed by

HPLC analysis of the mixture (*Waters Nova Pak C18* column; 23% MeCN in 0.1M aq. soln. of AcONH₄), hydrolysis of the glycosidic bond was completed within 6 h. The mixture was concentrated to ca. 2 ml and subjected to prep. HPLC separation (*Waters RCM Nova Pak* column, 24 × 10; 10% MeCN in 0.1M aq. soln. of AcONH₄). Fractions containing pure product were combined, evaporated to dryness, and desalted by repeated chromatography on a short reversed-phase silica-gel column following by a counter-ion exchange on *Dowex Cl⁻* column. The final eluate was concentrated to a small volume and the freeze-dried to give **3** as a pale yellow powder (228 mg, 87% yield). UV (H₂O): 250 (10100), 389 (8400). ¹H-NMR (D₂O): 10.40 (H–C(5)); 9.01 (H–C(8)); 8.90 (H–C(7)); 8.59 (H–C(6)); 8.51 (H–C(3)); 4.33 (MeO). ¹³C-NMR (D₂O): 162.26 (C(1)); 156.20 (C(3)); 155.95 (C(9)); 147.20 (C(7)); 139.12 (C(8a)); 134.95 (C(5)); 134.07 (C(4a)); 130.19 (C(6)); 126.14 (C(8)); 118.21 (C(10a)); 57.2 (MeO). Anal. calc. for C₁₁H₁₀N₅OCl: C 50.11, H 3.82, N 26.56; found: C 49.84, H 3.71, N 25.76.

REFERENCES

- [1] B. Skalski, J. Bartoszewicz, S. Paszyc, Z. Gdaniec, R. W. Adamiak, *Tetrahedron* **1987**, *43*, 3955.
- [2] B. Skalski, S. Paszyc, R. W. Adamiak, R. P. Steer, R. E. Verrall, *J. Chem. Soc., Perkin Trans. 2* **1989**, 1691.
- [3] S. Mielewicz, G. Dominiak, Z. Gdaniec, E. Krzymanska-Olejnik, R. W. Adamiak, B. Skalski, *Nucleosides Nucleotides* **1991**, *10*, 263.
- [4] S. Jayaraman, L. Teitler, B. Skalski, A. S. Verkman, *Am. J. Physiol. (Cell Physiol.)* **1999**, *277*(46), C1008.
- [5] A. Burdzy, B. Skalski, S. Paszyc, Z. Gdaniec, R. W. Adamiak, *Nucleosides Nucleotides* **1998**, *17*, 143.
- [6] R. F. Steiner, Y. Kubota, 'Fluorescent Dye-Nucleic Acid Complexes', in 'Excited States of Biopolymers', Ed. R. F. Steiner, Plenum Press, New York, 1983; D. Suh, J. B. Chaires, *Bioorg. Med. Chem.* **1995**, *3*, 723.
- [7] S. Georghiou, *Photochem. Photobiol.* **1977**, *26*, 59; J. Pastor, J. G. Siro, J. L. Garcia-Navio, J. J. Vaquero, J. Alvarez-Builla, F. Gago, B. de Pascual-Teresa, M. Pastor, M. M. Rodrigo, *J. Org. Chem.* **1997**, *62*, 5476.
- [8] J. R. Lakowicz, 'Principles of Fluorescence Spectroscopy', 2nd edn., Kluwer Academic/Plenum Publishers, New York, 1999, p. 243.
- [9] Y. Kubota, Y. Motoda, Y. Shigemune, Y. Fujisaki, *Photochem. Photobiol.* **1978**, *29*, 1099.
- [10] C. A. M. Seidel, A. Schulz, M. H. M. Sauer, *J. Phys. Chem.* **1996**, *100*, 5541.
- [11] G. Scatchard, *Ann. N.Y. Acad. Sci.* **1949**, *51*, 660.
- [12] W. Müller, D. M. Crothers, *Eur. J. Biochem.* **1975**, *54*, 267.
- [13] D. E. V. Schmechel, D. M. Crothers, *Biopolymers* **1971**, *10*, 465; J.-B. LePecq, C. Paoletti, *J. Mol. Biol.* **1967**, *27*, 87.
- [14] C. V. Kumar, E. H. Asuncion, *J. Am. Chem. Soc.* **1993**, *115*, 8547.
- [15] S. R. Meech, D. Phillips, *J. Photochem.* **1983**, *23*, 193.
- [16] J. K. Barton, J. M. Goldberg, C. V. Kumar, N. J. Turro, *J. Am. Chem. Soc.* **1986**, *108*, 2081.

Received June 11, 2001